Received February 25, 2021, accepted March 21, 2021, date of publication March 29, 2021, date of current version April 7, 2021.

Digital Object Identifier 10.1109/ACCESS.2021.3069247

Enhancing Spectrum Efficiency for Multiple Users in Hybrid Satellite-Terrestrial Networks

NHAT-TIEN NGUYEN[1], HONG-NHU NGUYEN[1], NGOC-LONG NGUYEN[1], ANH-TU LE[2], DINH-THUAN DO[3], (Senior Member, IEEE), AND MIROSLAV VOZNAK[1], (Senior Member, IEEE)

[1]Department of Telecommunications, VSB-Technical University of Ostrava, 70833 Ostrava, Czech Republic
[2]Faculty of Electronics Technology, Industrial University of Ho Chi Minh City (IUH), Ho Chi Minh City 700000, Vietnam
[3]Department of Computer Science and Information Engineering, Asia University, Taichung 41354, Taiwan

Corresponding author: Dinh-Thuan Do (dodinhthuan@asia.edu.tw)

The research leading to this results was supported by the Czech Ministry of Education, Youth and Sports under project reg. no. SP2020/65 and SP2021/25, and also partially from the Large Infrastructures for Research, Experimental Development and Innovations project ''e-Infrastructure CZ'' reg. no. LM2018140.

ABSTRACT In the paper, we present a study on the performance analysis of a non-orthogonal multiple access (NOMA) underlay cognitive hybrid satellite-terrestrial relaying network (CSTRN) and highlight the performance gaps between multiple users. The satellite source communicates with users by enabling cognitive radio scheme to forward signals to secondary destinations on the ground which belong to dedicated groups following the principle of NOMA. In this scenario, the secondary source acts a relay and employs Amplify and Forward (AF) mode to serve distant NOMA users under a given interference constraint. To characterize the transmission environment, the shadowed-Rician fading and Nakagami-*m* fading models are widely adopted to the relevant hybrid channels. To provide detailed examination of the system performance metrics, we aim to derive closed-form formulas for the outage probability of the secondary destinations in the presence of the primary interference power constraint imposed by the adjacent primary satellite network. Finally, our simulation results showed that a greater number of antennas, better quality of wireless channels and power allocation factors exhibit the main effects on system performance.

INDEX TERMS Non-orthogonal multiple access, cognitive hybrid satellite-terrestrial relaying network, cognitive radio.

I. INTRODUCTION

Regarded as an attractive method for achieving high throughput with a broad coverage area, hybrid satellite systems and terrestrial networks can be integrated to form hybrid satellite terrestrial networks (HSTNs) [1]. In a HSTN, a wide range of applications can be offered for the purposes of navigation, broadcasting and disaster relief [2]. To improve coverage, system performance can be achieved in the system models by employing cooperative relaying techniques which are reported in [3], [4]. In addition, both the relaying network and cognitive radio (CR) technology can benefit to major applications of HSTNs by enhancing the efficiency of spectrum utilization. The promising architecture is studied as cognitive HSTN (CHSTN) [5]–[10]. In such a CHSTN, a secondary terrestrial network is permitted to operate in the same spectrum resource as the primary satellite network. The two main factors in CHSTNs, i.e. secondary user (SU) transmit power constraints and inefficient use of available spectrum resources, may degrade the performance of the secondary network.

Because data traffic is ever rapidly growing, it is crucial to study new multiple access methods. There are other challenges since current communication systems possess limited power and spectrum resources. Fortunately, existing systems can potentially overcome these challenges by enabling the recently proposed non-orthogonal multiple access (NOMA). Unlike conventional orthogonal multiple access (OMA), NOMA-aided base stations employ the power domain to assist multiplexing of multiple users before sending to mobile users. The NOMA technique, superposition coding (SC) and successive interference cancellation (SIC) performed at the corresponding transmitters and receivers allow users to achieve higher spectrum efficiency [11]. In the principle of NOMA, more power levels are allocated to users with poorer channels. As such, weak users can decode signals

The associate editor coordinating the review of this manuscript and approving it for publication was Fang Yang.

directly by considering other signals, such as noise. Before detecting the main signal, the user which experiences a better channel decodes the strong signals and eliminates them. The NOMA technique has three main benefits: low latency, massive connectivity, and high spectral efficiency [12]. The authors in [13] investigated a downlink NOMA scenario with randomly deployed users to demonstrate its superior performance, i.e. ergodic capacity. The authors in [14] studied a real scenario with a transmitter that only achieved statistical channel state information (CSI) associated with each user. They proposed this model to implement a NOMA system by employing the Nakagami-m fading channels as a practical downlink. The authors in [15] presented the capability of unmanned aerial vehicle (UAV) communications employing full-duplex NOMA (FD-NOMA) to enhance spectrum utilization. They described closed-form outage probability formulas for several scenarios such as FD-NOMA, half-duplex NOMA (HD-NOMA), and half-duplex OMA (HD-OMA) schemes over Rician shadowed fading channels. The authors in [16] studied an interesting alternative to conventional power domain-NOMA, known as NOMA-2000, in which multiple access was implemented by applying two sets of orthogonal waveforms. The simulation results in [17] for a fair-NOMA approach reported that each user's capacity was greater than or equal to the capacity of a system relying on OMA. Recent studies such as [18], [19] have also developed the application of device-to-device (D2D) communication in the context of NOMA. A cooperative NOMA scheme was studied in [20]–[23] to increase reliability and coverage. Users experiencing better channels were treated as relays to forward the messages of distant users experiencing poorer channels. The authors in [24] and [25] proposed a UAV-NOMA network architecture. The authors in [25] indicated that D2D can be used to increase file dispatching efficiency. In a D2D-enhanced UAV-NOMA network, ground users (GUEs) may reuse the time-frequency resources assigned to NOMA links to share with other GUEs. The study in [26] presented two practical schemes of downlink UAV-NOMA. The first method minimized the transmit power of the UAV, satisfying the minimum achievable rate requirements. The second proposed method maximized the achievable rate of a specific user while maintaining the minimum achievable rate requirements for other users.

To further improve the efficiency of spectrum utilization, NOMA can gain more benefit from cognitive radio (CR) and forming CR-inspired NOMA scenarios [27]–[30]. The work in [27] investigated the integration of NOMA with CR to introduce more intelligent spectrum sharing paradigms. To examine the performance of secondary NOMA users, end-to-end outage probability is considered as the main performance metric. The recent work in [28] studied error rate performance in a scenario of relay-assisted NOMA with partial relay selection applied in an underlay CR network. Based on this system model, K relays were used to support transmission between secondary NOMA users and a secondary base station (SBS). In such a system, the relay which experiences the strongest link with the SBS is selected to forward the received signals to secondary receivers.

A. RELATED WORK

The authors in [31] considered the performance of an overlay cognitive hybrid satellite-terrestrial relaying network (CSTRN). This system contains a primary satellite transmitter set up to send signals to multiple terrestrial receivers and a secondary transmitter-receiver pair located on the ground. The primary satellite transmitter employing NOMA architecture to serve all users simultaneously. To deal with spectrum access, the secondary transmitter assisted primary communication through a cooperative relaying method. The authors in [32] studied the widely adopted shadowed-Rician fading and Nakagami-m fading models for relevant hybrid channels. Their main results were the derivation of a closed-form formula for the outage probability of a secondary network by considering the conditions on primary interference power constraints associated with the adjacent primary satellite network. The system reported in [33] introduced two main performance metrics: closed-form outage probability and approximate ergodic capacity expressions for the primary user (PU) and secondary user (SU). In this system, generalized Shadowed-Rician fading and a Nakagami-m fading were applied to satellite links and terrestrial links, respectively. The simulation results verified the superiority of NOMA compared to conventional OMA schemes by varying certain key parameters. The authors in [34] presented the critical effect of hardware impairments (HIs) at user devices in an overlay cognitive hybrid terrestrial network which included a primary satellite source–receiver pair and a secondary transmitter–receiver pair on the ground. To mitigate the effect of HIs, the authors studied an adaptive relaying (AR) protocol for both amplify-and-forward (AF) and decode-and-forward (DF) modes and compared its performance to competitor fixed relaying schemes.

However, the most benefit of NOMA in the CSTRN system is enabler of multiple served users in dedicated group of group. This paper motivated by recent studies [31]–[34] to highlight how we benefit from enabling CR and NOMA in the CSTRN system.

B. OUR CONTRIBUTION AND ORGANIZATION

The key findings of this paper can be summarized as follows:

- This study aims to propose a framework of multiple NOMA user in the CSTRN system by exploiting set of analytical expressions to indicate the system performance metrics. In particular, we consider the outage probability (OP) and throughput of a complicated system which is designed with enablers of NOMA, CR, multiple secondary users and multiple-antenna satellite.
- Although reference [31] quantified the performance of a NOMA-assisted the CSTRN of the primary and secondary networks in terms of outage probability by considering the pertinent heterogeneous fading models, our

TABLE 1. Comparison of proposed system with related works.

Context	Cooperative Relay Network	Multiple Antenna	NOMA	Multiple user	Asymptotic
This Work	Yes	Yes	Yes	Yes	Yes
[31]	Yes	No	Yes	Yes	Yes
[32]	No	No	Yes	No	No
[33]	Yes	No	Yes	No	No
[34]	Yes	No	No	No	No

study mentions on complicated scenario of multiple antennas at the satellite and multiple users in a considered group. It is beneficial to improvement performance of NOMA-assisted the CSTRN. Due to complicated results computed in studies related to CSTRN system [31]– [34], we also investigate the approximation performance of such outage behavior to look insights of such system. This important finding should be guidelines to design NOMA-CSTRN in practice. Table 1 should emphasize our key findings compared with recent studies.

- Our numerical simulations are expected to provided main parameters which are used to improve specific performance metrics for the NOMA-CSTRN. These parameters are power allocation factors, the number of transmit antennas, channel fading gains, and transmit signal-to-noise ratio at the satellite.

The other parts of the paper can be emphasized as follows. Section II presents the details of the system model along with computation of received signals and channel distributions. Section III considers main metric, namely outage probability and asymptotic computation of such performance metric. Section IV presents the numerical results and discussion. Finally, Section V intends to provide concluding remarks and outlines of future research directions.

II. SYSTEM MODEL

In the present study, we examine a satellite (S) equipped N_S antennae, a single antenna secondary relay (R), K secondary terrestrial destinations $D_k (1 \leqslant k \leqslant K)$ and a single primary terrestrial destination (PD). The key parameters and denotations can be seen in Table 2.

Two phases are required to process overall communication of a secondary network in such CSTRN. In the first phase, the superposition signal $s = \sum_{i=1}^{K} \sqrt{P_S \phi_i} x_i$ is sent from the S to the R using a weight vector $\mathbf{w}_{SR}$. The received signal at R is given by

$$y_R = \mathbf{h}_{SR}^{\dagger} \mathbf{w}_{SR} \sum_{i=1}^{K} \sqrt{P_S \phi_i} x_i + n_R, \tag{1}$$

where $\mathbf{h}_{SR} = \left[h_{SR}^1 \cdots h_{SR}^{N_S} \right]^T$ and n_R is the additive white Gaussian noise (AWGN) with $n_R \sim \mathcal{CN}(0, N_0)$. By employing a maximum ratio transmission (MRT) scheme [35],

TABLE 2. The descriptions of symbols.

Symbol	Description
N_S	Number of antennas at satellite
K	Number of terrestrial destination
P_S	The transmit power at S
P_R	The transmit power at R
x_i	The information required by destination i
ϕ_i	The power allocation coefficient
$\mathbf{h}_{Sv}$	The $N_S \times 1$ channel vector between satellite and relay with $v \in (R, P)$
h_{RD_k}	The channel coefficient between relay and terrestrial destination
h_{RP}	The channel coefficient between relay and primary user
$\lVert \bullet \rVert_F$	The Frobenius norm
$(\bullet)^{\dagger}$	The Conjugate transpose
$\beta(.,.)$	The Beta function
$\Gamma(.)$	The gamma function
$\gamma(.,.)$	The lower incomplete gamma function
${}_1F_1\,(.;.;.)$	The confluent hypergeometric function of the first kind
$G_{1,1}^{1,1}\,[.]$	The Meijer's G-function

the transmit beamforming vector is formulated as $\mathbf{w}_{SR} = \frac{\mathbf{h}_{SR}}{\lVert \mathbf{h}_{SR} \rVert_F}$.

After signal processing in the first phase, the R first amplifies the received signal y_R with a gain factor G. This variable gain is defined as $G = \sqrt{\frac{1}{P_S Z_R + N_0}}$, $Z_R = \lVert \mathbf{h}_{SR} \rVert_F^2$. Then, R forwards the processed signal to all distant users. The received signal at the kth user is given by

$$\begin{aligned} y_{D_k} &= \sqrt{P_R} h_{RD_k} G y_R + n_{D_k} \\ &= G h_{RD_k} \mathbf{h}_{SR}^{\dagger} \mathbf{w}_{SR} \sum_{i=1}^{K} \sqrt{P_S P_R \phi_i} x_i \\ &\quad + G \sqrt{P_R} h_{RD_k} n_R + n_{D_k}, \end{aligned} \tag{2}$$

Without loss of generality, the channel gains from R to D_k are ordered $h_{RD_1} \leqslant h_{RD_2} \leqslant \cdots \leqslant h_{RD_K}$. This ordering procedure is associated with NOMA requirements. $n_{D_k} \sim \mathcal{CN}(0, N_0)$ is the AWGN.

To prevent interference at the primary user beyond an acceptable level Q, the transmit power at S and R are given by [36] $P_S = \frac{Q}{Z_P}$ and $P_R = \frac{Q}{|h_{RP}|^2}$, respectively, where $Z_v = \lVert \mathbf{h}_{Sv} \rVert_F^2$, $v \in \{R, P\}$.

Considering how the system precisely detects the required signal at each user, we mention SIC in the context of NOMA. Since the desired signal encounters interference from the other users' signals, SIC is required at each user to eliminate

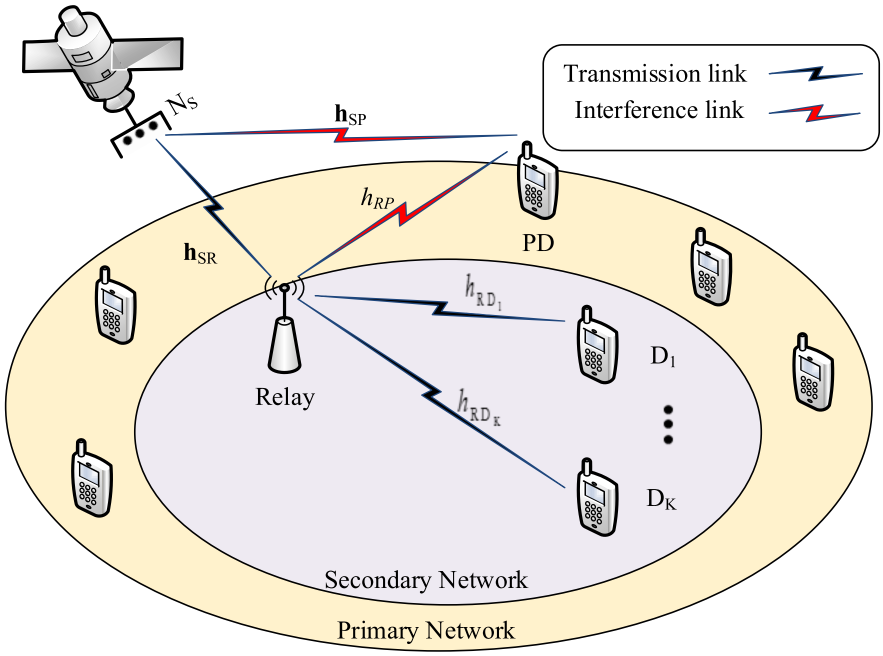

FIGURE 1. The system model of NOMA-CSTRN.

the adverse effect of inter-user interference. Therefore, at the k-th user, the m-th user's signal, $k < m$, must be detected. The system then deletes it from the received signal of the k-th user in a successive manner. In this situation, the m-th user's signal is treated as noise at the k-th user. We can therefore compute the signal-to-interference-and-noise ratio (SINR) for the k-th user to decode the m-th user's signal, $k \leqslant m$, as follows

$$\begin{aligned}\Gamma_{m\to k} &= \frac{G^2 P_R P_S Z_R |h_{RD_k}|^2 \phi_m}{G^2 P_R P_S Z_R |h_{RD_k}|^2 \sum\limits_{i=m+1}^{K} \phi_i + G^2 \sqrt{P_R} |h_{RD_k}|^2 N_0 + N_0} \\ &= \frac{\gamma_R \gamma_k \phi_m}{\gamma_R \gamma_k \sum\limits_{i=p+1}^{K} \phi_i + \gamma_k + \gamma_R + 1}, \end{aligned} \tag{3}$$

where $\rho = \frac{Q}{N_0}$, $\gamma_R = \rho Z_R / Z_P$ and $\gamma_k = \rho |h_{RD_k}|^2 / |h_{RP}|^2$. If x_m can be detected successfully, signal x_m can be deleted before the signal for user D_k is detected. The SINR of D_k to decode its own signal is given by

$$\Gamma_k = \frac{\gamma_R \gamma_k \phi_k}{\gamma_R \gamma_k \sum\limits_{i=k+1}^{K} \phi_i + \gamma_k + \gamma_R + 1}. \tag{4}$$

For successive processing of many users, the standard SIC component is operated until all other users' signals are detected. For the final user, the SINR of D_K to decode its own signal can be computed according to

$$\Gamma_K = \frac{\gamma_R \gamma_K \phi_K}{\gamma_K + \gamma_R + 1}. \tag{5}$$

In terms of the characteristics of wireless channels, the channel vector $\mathbf{h}_{Sv}$ is associated with i.i.d. Shadowed-Rician fading entries. By denoting $\delta_v = \Omega_{Sv} / (2b_{Sv})(2b_{Sv} m_{Sv} + \Omega_{Sv})$ in which m_{Sv} represents the fading severity parameter, Ω_{Sv} and b_{Sv} are the average power of Line-of-Sight (LOS) and multipath components, respectively, and ${}_1F_1(.;.;.)$ is the confluent hypergeometric function of the first kind [37, Eq. 9.210.1], the probability density function (PDF) of the squared amplitude of the channel coefficient $\left|h_{Sv}^{(i)}\right|^2$ is given by [4], [35]

$$f_{\left|h_{Sv}^{(i)}\right|^2}(x) = \alpha_v e^{-\beta_v x} {}_1F_1(m_{Sv}; 1; \delta_v x), x > 0, \tag{6}$$

where $\alpha_v = (2b_{Sv} m_{Sv} / (2b_{Sv} m_{Sv} + \Omega_{Sv}))^{m_{Sv}} / 2b_{Sv}$, $\beta_v = 0.5 b_{Sv}$. For Shadowed-Rician fading with integer-valued severity parameters, we can therefore rewrite (6) as

$$f_{\left|h_{Sv}^{(i)}\right|^2}(x) = \alpha_v \sum_{\kappa=0}^{m_{Sv}-1} \zeta_v(\kappa) x^\kappa e^{-\Psi_v x}, \tag{7}$$

where $\zeta_v(\kappa) = (-1)^\kappa (1 - m_{Sv})_\kappa \delta_v^\kappa / (\kappa!)^2$, $\Psi_v = \beta_v - \delta_v$ and $(.)_\kappa$ is the Pochhammer symbol [37, p. xliii], the PDF of Z_v under i.i.d. Shadowed Rician fading is given as

$$f_{Z_v}(x) = \sum_{i_1=0}^{m_{Sv}-1} \cdots \sum_{i_{N_S}=0}^{m_{Sv}-1} \Theta(v, N_S) x^{\Delta_v - 1} e^{-\Psi_v x}, \tag{8}$$

where

$$\Theta(v, N_S) = \alpha_v^{N_S} \prod_{\ell=1}^{N_S} \zeta_v(i_\ell) \prod_{j=1}^{N_S-1} \text{ß}\left(\sum_{l=1}^{j} i_l + j, i_{j+1} + 1\right), \tag{9a}$$

$$\Delta_v = \sum_{q=1}^{N_S} i_q + N_S. \tag{9b}$$

and ß(.; ,) is the Beta function [37, Eq. 8.384.1].

The cumulative distribution functions (CDF) of Z_v can be obtained as [37, Eq. 3.351.2]

$$F_{Z_v}(x) = 1 - \sum_{i_1=0}^{m_{Sv}-1} \cdots \sum_{i_{N_S}=0}^{m_{Sv}-1} \Theta(v, N_S) \times \sum_{p=0}^{\Delta_v-1} \frac{\Gamma(\Delta_v)\Psi_v^{-\Delta_v+p}}{p!} x^p e^{-\Psi_v x}. \tag{10}$$

Considering the characterization of Nakagami-m fading, the PDF and CDF of channel gain $\left|\tilde{h}_{RD_k}\right|^2$ are given, respectively, by [38]

$$f_{\left|\tilde{h}_{RD_k}\right|^2}(x) = \frac{x^{m_D-1}}{\Gamma(m_D)\lambda_D^{m_D}} e^{-\frac{x}{\lambda_D}}, \tag{11}$$

and

$$F_{\left|\tilde{h}_{RD_k}\right|^2}(x) = \frac{\gamma(m_D, x/\lambda_D)}{\Gamma(m_D)} = 1 - e^{-\frac{x}{\lambda_D}} \sum_{n_D=0}^{m_D-1} \frac{x^{n_D}}{\lambda_D^{n_D} n_D!}, \tag{12}$$

where $\lambda_D = \frac{\Omega_D}{m_D}$, m_D and $\Omega_D = \Omega_1 = \Omega_2 = \cdots = \Omega_K$ in this case are the fading severity and average power, respectively, and $\gamma(.,.)$ is the lower incomplete gamma function [37, Eq. 8.350.1]. Using order statistics, the PDF of $\left|h_{RD_k}\right|^2$ can be represented as

$$\begin{aligned} f_{|h_{RD_k}|^2}(x) &= \Upsilon f_{\left|\tilde{h}_{RD_k}\right|^2}(x)\left[F_{\left|\tilde{h}_{RD_k}\right|^2}(x)\right]^{k-1} \times \left[1 - F_{\left|\tilde{h}_{RD_k}\right|^2}(x)\right]^{K-k} \\ &= \Upsilon \sum_{m=0}^{K-k} (-1)^m \binom{K-k}{m} \times f_{\left|\tilde{h}_{RD_k}\right|^2}(x)\left[F_{\left|\tilde{h}_{RD_k}\right|^2}(x)\right]^{k+m-1}, \end{aligned} \tag{13}$$

where $\Upsilon = \frac{K!}{(K-k)!(k-1)!}$. Furthermore, the CDF of $|h_{RD_k}|^2$ is expressed as

$$F_{|h_{RD_k}|^2}(x) = \Upsilon \sum_{m=0}^{K-k} \binom{K-k}{m} \frac{(-1)^m}{k+m} \left[F_{\left|\tilde{h}_{RD_k}\right|^2}(x)\right]^{k+m}. \tag{14}$$

The PDF and CDF of $|h_{RP}|^2$ are computed, respectively, according to

$$f_{|h_{RP}|^2}(x) = \frac{x^{m_{RP}-1}}{\Gamma(m_{RP})\lambda_{RP}^{m_{RP}}} e^{-\frac{x}{\lambda_{RP}}}, \tag{15}$$

and

$$F_{|h_{RP}|^2}(x) = \frac{\gamma(m_{RP}, x/\lambda_D)}{\Gamma(m_{RP})} = 1 - e^{-\frac{x}{\lambda_{RP}}} \sum_{n_{RP}=0}^{m_{RP}-1} \frac{x^{n_{RP}}}{\lambda_{RP}^{n_{RP}} n_{RP}!}, \tag{16}$$

where $\lambda_{RP} = \frac{\Omega_{RP}}{m_{RP}}$, m_{RP} is the fading severity, and Ω_{RP} represents the average power.

III. SYSTEM PERFORMANCE ANALYSIS

A. OUTAGE PROBABILITY

The main performance metric, i.e. outage probability, requires study. In this case, the SIC is applied to many users. In particular, SIC is performed at the k-th user in two steps. The first and the second steps correspond to detecting and canceling the m-th user's signal ($m \leqslant k$). The intended users are then able to decode its own signal. In an unwanted scenario, the k-th user cannot detect the k-th user's signal and outage occurs. It is denoted by $E_{k,m}$. In particular, the outage probability of the k-th user is given by[1]

$$\mathcal{OP}_k^{out} = 1 - \Pr\left(E_{k,1}^c \cap \ldots \cap E_{k,k}^c\right), \tag{17}$$

where $E_{k,m}^c$ is the complement event of $E_{k,m}$. It can be written as

$$\begin{aligned} E_{k,m}^c &= \left[\frac{\gamma_R \gamma_k \phi_m}{\gamma_R \gamma_k \sum_{i=p+1}^{K} \phi_i + \gamma_k + \gamma_R + 1} > \gamma_m\right] \\ &\overset{(a)}{=} \left[\gamma_k > \delta_m, \gamma_R > \frac{\delta_m(\gamma_k+1)}{\gamma_k - \delta_m}\right], \end{aligned} \tag{18}$$

where $\gamma_m = 2^{R_m} - 1$, R_m is the target rate at the m-th user, $\delta_m = \frac{\gamma_m}{\phi_m - \gamma_m \sum_{i=p+1}^{K} \phi_i}$, and step (a) follows as $\phi_m > \gamma_m \sum_{i=p+1}^{K} \phi_i$. We can then rewrite:

$$OP_k^{out} = 1 - \Pr\left(\gamma_k > \delta_k^*, \gamma_R > \frac{\delta_k^*(\gamma_k+1)}{\gamma_k - \delta_k^*}\right), \tag{19}$$

where $\delta_k^* = \underbrace{\max}_{1 \leqslant m \leqslant k} \delta_m$.

Proposition 1: The CDF of γ_R is obtained as

$$F_{\gamma_R}(x) = 1 - \widetilde{\sum}(R, P) \times \sum_{p=0}^{\Delta_R-1} \frac{\Gamma(\Delta_R)\Gamma(\Delta_P+p)\Psi_R^{-\Delta_R+p}\rho^{\Delta_P}x^p}{p!(\Psi_R x + \rho\Psi_P)^{\Delta_P+p}}. \tag{20}$$

[1] Although derivations of outage probability have studied in most of paper, such metric is still necessary to evaluate quality of links in term of satellite and devices in ground. Further, since the characteristic of SINR of multiple users limit us to consider other metric, we still aim to find insights in next sections.

where

$$\widetilde{\sum}(R,P)=\sum_{i_1=0}^{m_{SR}-1}\cdots\sum_{i_{N_S}=0}^{m_{SR}-1}\Theta(R,N_S)\times\sum_{i_1=0}^{m_{SP}-1}\cdots\sum_{i_{N_S}=0}^{m_{SP}-1}\Theta(P,N_S) \quad (21)$$

Proof: See Appendix A.

Since $\gamma_k = \rho|h_{RD_k}|^2/|h_{RP}|^2$ as the ratio of two Gamma random variables, we can derive the PDF of γ_k with $x > 0$ as

$$F_{\gamma_k}(x) = 1-\sum_{m=0}^{K-k}\sum_{a=0}^{k+m}\sum_{b=0}^{a(m_D-1)}\binom{K-k}{m}\binom{k+m}{a}\times\frac{\Upsilon\Gamma(m_{RP}+b)(-1)^{m+a}\vartheta_b(a)}{(k+m)\Gamma(m_{RP})}\times\frac{x^b\rho^{m_{RP}}\lambda_{RP}^b(\lambda_D)^{m_{RP}+b}}{(a\lambda_{RP}x+\rho\lambda_D)^{m_{RP}+b}}. \quad (22)$$

By taking the first derivative of (22), the corresponding PDF can be obtained as

$$f_{\gamma_k}(x) = \Upsilon\sum_{m=0}^{K-k}\sum_{a=0}^{k+m-1}\sum_{b=0}^{a(m_D-1)}\binom{K-k}{m}\binom{k+m-1}{a}\times\frac{\vartheta_b(a)(-1)^{m+a}\Gamma(m_{RP}+m_D+b)}{\Gamma(m_D)\Gamma(m_{RP})}\times\frac{\rho^{m_{RP}}\lambda_{RP}^{m_D+b}\lambda_D^{m_{RP}+b}x^{m_D+b-1}}{(\lambda_D\rho+\lambda_{RP}(a+1)x)^{m_{RP}+m_D+b}} \quad (23)$$

Proposition 2: The closed-form formula of $\mathcal{OP}_{out}$ of the k-th user is given by (24), shown at the bottom of the next page.

Proof: See Appendix B.

Remark 1: Since (24) *contains lots of main parameters, the considered system performance relies on quality of channels and transmit SNR at the satellite, interference power constraint. We treat system performance of small group of users as basic requirement to retain normal operation. However, it is still challenging task to know how large the number of users in dedicated group the system can serve. We expect to further give suggestions in the section of numerical simulation.*

B. ASYMPTOTIC OUTAGE PROBABILITY AND DIVERSITY ORDER ANALYSIS

To gain more insight into CSTRN performance, the asymptotic outage probability should be considered in the high SNR region ($\rho \to \infty$). Interestingly, when $\rho \to \infty$ we can apply the Maclaurin series expansion of the exponential function in (7) to approximate. The PDF of ρZ_R is then given as

$$f_{\rho Z_R}(x) \simeq \frac{\alpha^{N_S}}{(N_S-1)!\rho^{N_S}}x^{N_S-1}, \quad (25)$$

and the corresponding CDF follows asymptotic behavior according to

$$F_{\rho Z_R}(x) \simeq \frac{\alpha^{N_S}}{(N_S)!\rho^{N_S}}x^{N_S}. \quad (26)$$

Hence, substituting (26) and (8) into (32) and together with [37, Eq. 3.351.3], the asymptotic CDF of γ_R is obtained as follows

$$F_{\gamma_R}(x) \simeq \sum_{i_1=0}^{m_{SP}-1}\cdots\sum_{i_{N_S}=0}^{m_{SP}-1}\Theta(P,N_S)\times\frac{\alpha^{N_S}x^{N_S}(N_S+\Delta_P-1)!}{(N_S)!\rho^{N_S}(\Psi_P)^{N_S+\Delta_P}}. \quad (27)$$

Similarly, by applying the Maclaurin series representation of the exponential function, the CDF of ρY can be obtained as

$$F_{\rho|h_{RD_k}|^2}(x) \simeq \frac{1}{[\Gamma(m_D+1)]^K}\left(\frac{x}{\lambda_D\rho}\right)^{m_DK}. \quad (28)$$

Assisted by (30) and (15), the asymptotic behavior of γ_Y is written as

$$F_{\gamma_k}(x) \simeq \frac{\Gamma(m_DK+m_{RP})}{[\Gamma(m_D+1)]^K\Gamma(m_{RP})}\left(\frac{x\lambda_{RP}}{\lambda_D\rho}\right)^{m_DK} \quad (29)$$

With a large SNR, we can rewrite $\Gamma_{RD} \simeq \frac{\gamma_R\gamma_Y}{\gamma_R+\gamma_Y}$, and hence, system performance is dominated by the weakest link. We can thus represent the asymptotic OP as

$$OP_k^{out,\rho\to\infty} \simeq \sum_{i_1=0}^{m_{SP}-1}\cdots\sum_{i_{N_S}=0}^{m_{SP}-1}\Theta(P,N_S)\times\frac{\alpha^{N_S}(\delta_k^*)^{N_S}\Gamma(N_S+\Delta_P)}{(N_S)!\rho^{N_S}(\Psi_P)^{N_S+\Delta_P}}+\frac{\Gamma(N_Dm_DK+m_{RP})}{[\Gamma(m_D+1)]^K\Gamma(m_{RP})}\left(\frac{\delta_k^*\lambda_{RP}}{\lambda_D\rho}\right)^{m_DK} \quad (30)$$

It is straightforward to indicate that when $\rho \to \infty$, the diversity order is $min(N_S, m_DK)$.

Remark 2: To evaluate the outage behavior, we conduct such asymptotic computations as helpful guideline of system design in practice. We aim to enhance the transmit SNR at the satellite and then to improve system performance of each user. Since SNR mainly depends on N_S, design of multiple antenna for satellite is highly demand to improve performance for users in ground compared with adjusting other system parameters. We expect to further verify such explanation in the section of numerical simulation.

C. THROUGHPUT

Based on outage probability, we can further evaluate throughput in delay-limited transmission mode. For a fixed target rate R_k, we can compute the overall throughput as follows [39]

$$T = \frac{1}{2}\sum_{k=1}^{K}R_k\left(1-OP_k^{out}\right). \quad (31)$$

TABLE 3. Satellite channel parameters.

Parameter	m_{Sv}	b_{Sv}	Ω_{Sv}
The heavy shadowing	1	0.063	0.007
The average shadowing	5	0.251	279

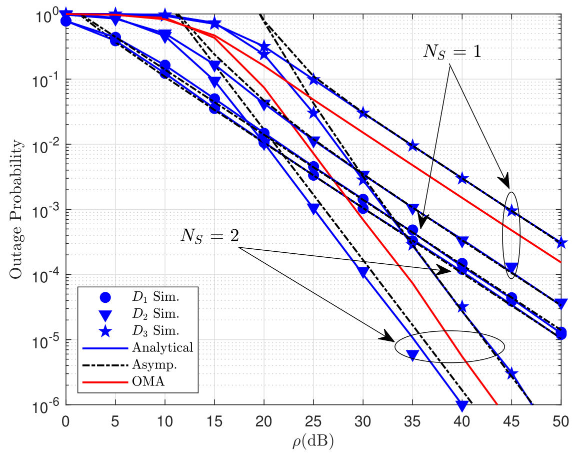

FIGURE 2. Outage probability versus transmit ρ varying N_S with $m = 1$ and satellite link in the HS scenario.

IV. NUMERICAL RESULTS

This section provides and discusses the numerical results. To verify the accuracy of the expressions, we compared the analytical results with Monte Carlo simulation results. Unless mentioned otherwise, we set $K = 3$, $\phi_1 = 0.5$, $\phi_2 = 0.4$, $\phi_3 = 0.1$, the target rate $R_1 = 0.1$, $R_2 = 0.5$ and $R_3 = 1$, and the main parameters before simulation as $m_D = m_{RP} = m$ and $\Omega_D = \Omega_{RP} = 1$. The Shadowed-Rician fading parameters for the satellite links are described in the Table 3.

Fig. 2 demonstrates the comparison of outage probability performance of three users by changing the number of satellite's antenna N_S. It can be intuitively seen that, by increasing N_S the considered system obviously improves the outage performance of three users. The first user D_1 shows its superiority in term of outage performance in case of single antenna at the satellite $N_S = 1$, then the worst performance occurs in user D_3 which is allocated less percentage of transmit power. The system based on OMA scheme shows its performance, but such outage behavior just better than user D_3. The main reason is that OMA-based system need more time slots to process the same number of users compared with NOMA-based system. It is valuable finding since Monte-Carlo based simulation and analytical result are matched very well. If we increase the number of antennas at the satellite, such performance metrics show its improvement which demonstrating

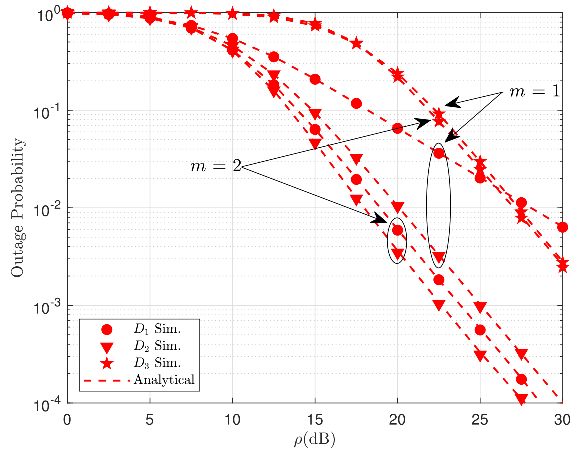

FIGURE 3. Outage probability versus transmit ρ varying m with $N_S = 2$ and satellite link in the HS scenario.

the benefits of introducing multiple antennas in the NOMA-CSTRN. Furthermore, asymptotic lines of outage probability match exact curves at high SNR regime which indicates the exactness of our derived expressions in term of outage probability.

Fig. 3 depicts the outage performance of the secondary users against two crucial parameters i.e., Nakagami channel parameter m with the number of transmit antennas set as $N_S = 2$. Similarly with previous figure, we can see significant improvement in term of outage behavior once SNR is greater than 25 dB. It can be explained that since the outage probability is a function of ρ, we can see that the outage probability decreases since ρ increases, shown in (4), (5), and (6). However, outage performance improves significantly for case of $m = 2$. Consequently, by improving quality of channels at ground, an increasing m will improve the outage performance of all users.

Fig. 4 illustrates the effect of different channel conditions about satellite link from S to R, the outage performance of these users can be improved when either the terrestrial link quality gets better, i.e. AS case is better case among two considered cases. In particular, comparing those analytical and asymptotic OP curves in Figs. 2 and Fig.3, we can see that asymptotic results agree with analytical results across the entire average SNR range.

As can be seen in Fig. 5 and Fig. 6 the throughput performance of such NOMA-CSTRN system can be improved by changing configurations of transmit antennas at the satellite and links from the satellite to base station at ground. From (31), it can be explained that further metric, throughput

$$\mathcal{OP}_k^{out} = 1 - \widetilde{\sum}(R,P) \sum_{p=0}^{\Delta_R-1} \sum_{m=0}^{K-k} \sum_{a=0}^{k+m-1} \sum_{b=0}^{a(m_D-1)} \sum_{l_1=0}^{p} \sum_{l_2=0}^{m_D+b+l_1-1} \binom{k+m-1}{a}\binom{K-k}{m}\binom{p}{l_1}\binom{m_D+b+l_1-1}{l_2}$$
$$\times \frac{\tilde{\Gamma}\Upsilon\vartheta_b(a)(-1)^{m+a}\left(\delta_k^*\right)^{p+m_D+b+l_1-l_2-1}\partial_3^{\Delta_P-m_{RP}-m_D-b+l_2+1}}{\Psi_R^{\Delta_R-p}\rho^{-\Delta_P-m_{RP}}\lambda_{RP}^{m_{RP}}\lambda_D^{-m_{RP}-b}\partial_1^{\Delta_P+p}(1+a)^{m_{RP}+m_D+b}} G_{2,2}^{2,2}\left[\partial_2\partial_3 \middle| \begin{matrix} -\Delta_P-l_2, 1-\Delta_P-p \\ m_{RP}+m_D+b-\Delta_P-l_2-1, 0 \end{matrix}\right] \quad (24)$$

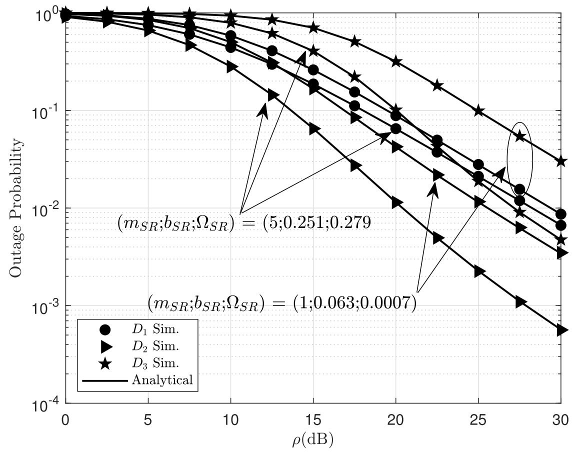

FIGURE 4. **Outage probability versus transmit ρ and varying satellite link from S to R with $N_S = m = 1$ and satellite link from S to PD in the HS scenario.**

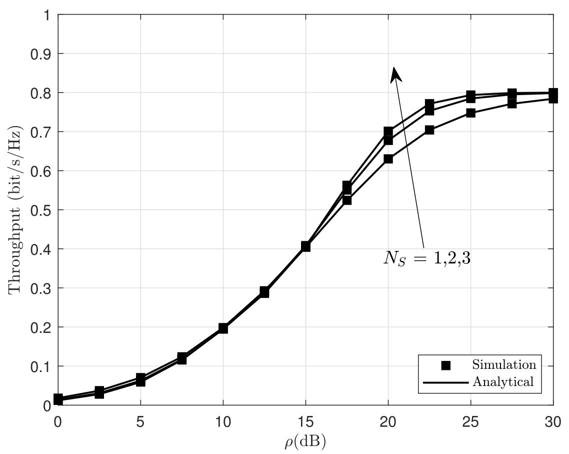

FIGURE 5. **System throughput versus transmit ρ and varying N_S with $m = 1$ and satellite link in the HS scenario.**

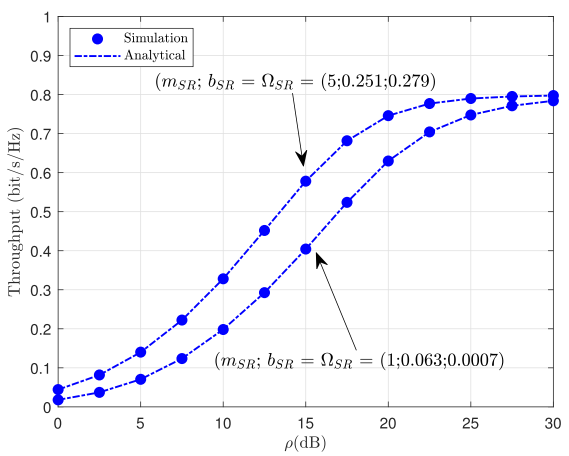

FIGURE 6. **System throughput versus transmit ρ and two kinds of satellite links from S to R (AS and HS) with $N_S = m = 1$.**

depends on the outage probability achieved in previous steps. Therefore, quality of channels results in the curves of the throughput of system. The higher value of N_S contributes to improve SINRs, then the higher throughput performance can be benefited. These observations become important guidelines to design such NOMA-CSTRN system.

V. CONCLUSION

This study has investigated the performance of an NOMA-CSTRN system wherein multiple secondary terrestrial users enjoys the access to spectrum with a primary satellite network to further achieve higher spectrum efficiency. Different from the current studies, we have considered the multiple antennas designed at the satellite and NOMA to indicate performance of several users which are groups in the context of NOMA scheme. We also consider throughput performance with different configurations of channels associated with transmission links and key parameters are necessary to improve performance metrics, i.e. outage probability and throughput. Above all, a comparison with many scenarios revealed that proposed NOMA-CSTRN system provides different performance for many users while utilizing the spectrum resource is conducted efficiently. Further metrics are expected to study in future work.

APPENDIX A

The CDF of γ_R can be rewritten as

$$\begin{aligned} F_{\gamma_R}(x) &= \Pr\left(Z_R < \frac{xZ_P}{\rho}\right) \\ &= \int_0^\infty f_{Z_P}(z) F_{Z_R}\left(\frac{xz}{\rho}\right) dz \\ &= 1 - \int_0^\infty f_{Z_P}(z)\left(1 - F_{Z_R}\left(\frac{xz}{\rho}\right)\right) dz. \end{aligned} \tag{32}$$

With the help of (8) and (10), we can express (32) as

$$\begin{aligned} F_{\gamma_R}(x) &= 1 - \widetilde{\sum}(R,P) \\ &\times \sum_{p=0}^{\Delta_R-1} \frac{\Gamma(\Delta_R)\Psi_R^{-\Delta_R+p}}{p!}\left(\frac{x}{\rho}\right)^p \\ &\times \int_0^\infty z^{\Delta_P+p-1} e^{-\left(\frac{\Psi_R x}{\rho}+\Psi_P\right)z} dz. \end{aligned} \tag{33}$$

Based on [37, Eq. 3.351], we obtain

$$\begin{aligned} F_{\gamma_R}(x) = 1 - \widetilde{\sum}(R,P) \\ \times \sum_{p=0}^{\Delta_R-1} \frac{\Gamma(\Delta_R)\Gamma(\Delta_P+p)\Psi_R^{-\Delta_R+p}\rho^{\Delta_P}x^p}{p!(\Psi_R x+\rho\Psi_P)^{\Delta_P+p}}. \end{aligned} \tag{34}$$

This is the end of the proof.

APPENDIX B

Then, we can calculate (19) as

$$\mathcal{OP}_k^{out} = 1 - \widetilde{\sum}(R,P) \sum_{p=0}^{\Delta_R-1} \sum_{m=0}^{K-k} \sum_{a=0}^{k+m-1} \sum_{b=0}^{a(m_D-1)}$$

$$\times \binom{k+m-1}{a}\binom{K-k}{m}\frac{\tilde{\Gamma}\Upsilon(-1)^{m+a}\vartheta_b(a)}{\Psi_R^{\Delta_R-p}}$$
$$\times \frac{\Gamma(\Delta_P+p)\,\Gamma(m_{RP}+m_D+b)\left(\delta_k^*\right)^p}{\rho^{-\Delta_P-m_{RP}}\lambda_{RP}^{-m_D-b}\lambda_D^{-m_{RP}-b}}$$
$$\times \int_{\delta_k}^{\infty} \frac{\left(x-\delta_k^*\right)^{\Delta_P}}{\left(\lambda_D\rho+\lambda_{RP}(a+1)x\right)^{m_{RP}+m_D+b}}$$
$$\times \frac{x^{m_D+b-1}(x+1)^p}{\left(\Psi_R\delta_k^*(x+1)+\rho\Psi_P\left(x-\delta_k^*\right)\right)^{\Delta_P+p}}, \quad (35)$$

where $\tilde{\Gamma} = \frac{\Gamma(\Delta_R)}{p!\Gamma(m_D)\Gamma(m_{RP})}$. Here, we apply the identity [40, Eq. 10]

$$(1+ax)^{-b} = \frac{1}{\Gamma(b)} G_{1,1}^{1,1}\left[ax \,\middle|\, \begin{matrix}1-b\\0\end{matrix}\right]. \quad (36)$$

where $G_{1,1}^{1,1}[.]$ denotes Meijer's G-function [37, Eq. 8.2.1.1]. Then, we represent (35) as

$$\mathcal{OP}_k^{out}$$
$$= 1 - \widetilde{\sum}(R,P) \sum_{p=0}^{\Delta_R-1}\sum_{m=0}^{K-k}\sum_{a=0}^{k+m-1}\sum_{b=0}^{a(m_D-1)}\sum_{l_1=0}^{p}\sum_{l_2=0}^{m_D+b+l_1-1}$$
$$\times \binom{k+m-1}{a}\binom{K-k}{m}\binom{p}{l_1}\binom{m_D+b+l_1-1}{l_2}$$
$$\times \frac{\Upsilon\tilde{\Gamma}\Gamma(m_{RP}+m_D+b)(-1)^{m+a}\vartheta_b(a)(\delta_k^*)^{p+m_D+b+l_1-l_2-1}}{\Psi_R^{\Delta_R-p}\rho^{-\Delta_P-m_{RP}}\lambda_{RP}^{m_{RP}}\lambda_D^{-m_{RP}-b}\partial_1^{\Delta_P+p}(1+a)^{m_{RP}+m_D+b}}$$
$$\times \int_0^{\infty}\frac{t^{\Delta_P+l_2}}{(\partial_3+t)^{m_{RP}+m_D+b}} G_{1,1}^{1,1}\left[\partial_2 t \,\middle|\, \begin{matrix}1-\Delta_P-p\\0\end{matrix}\right]dt, \quad (37)$$

where $\partial_1 = \Psi_R\delta_k^*\left(\delta_k^*+1\right)$, $\partial_2 = \frac{(\Psi_R\delta_k^*+\rho\Psi_P)}{\partial_1}$ and $\partial_3 = \frac{\lambda_D\rho+\lambda_{RP}(a+1)\delta_k^*}{\lambda_{RP}(a+1)}$. Based on [37, Eq. 7.811.5] and after some algebraic manipulation, we obtain (22).

This is the end of the proof.

REFERENCES

[1] W. Cao, Y. Zou, Z. Yang, and J. Zhu, "Relay selection for improving physical-layer security in hybrid satellite-terrestrial relay networks," *IEEE Access*, vol. 6, pp. 65275–65285, 2018.

[2] K. An, Y. Li, X. Yan, and T. Liang, "On the performance of cache-enabled hybrid satellite-terrestrial relay networks," *IEEE Wireless Commun. Lett.*, vol. 8, no. 5, pp. 1506–1509, Oct. 2019.

[3] D.-T. Do, "Optimal throughput under time power switching based relaying protocol in energy harvesting cooperative networks," *Wireless Pers. Commun.*, vol. 87, no. 2, pp. 551–564, Mar. 2016.

[4] V. Bankey, P. K. Upadhyay, D. B. Da Costa, P. S. Bithas, A. G. Kanatas, and U. S. Dias, "Performance analysis of multi-antenna multiuser hybrid satellite-terrestrial relay systems for mobile services delivery," *IEEE Access*, vol. 6, pp. 24729–24745, 2018.

[5] S. K. Sharma, S. Chatzinotas, and B. Ottersten, "Cognitive radio techniques for satellite communication systems," in *Proc. IEEE 78th Veh. Technol. Conf. (VTC Fall)*, Sep. 2013, pp. 1–5.

[6] S. Vassaki, M. I. Poulakis, A. D. Panagopoulos, and P. Constantinou, "Power allocation in cognitive satellite terrestrial networks with QoS constraints," *IEEE Commun. Lett.*, vol. 17, no. 7, pp. 1344–1347, Jul. 2013.

[7] Z. Li, F. Xiao, S. Wang, T. Pei, and J. Li, "Achievable rate maximization for cognitive hybrid satellite-terrestrial networks with AF-relays," *IEEE J. Sel. Areas Commun.*, vol. 36, no. 2, pp. 304–313, Feb. 2018.

[8] X. Zhang, K. An, B. Zhang, Z. Chen, Y. Yan, and D. Guo, "Vickrey auction-based secondary relay selection in cognitive hybrid satellite-terrestrial overlay networks with non-orthogonal multiple access," *IEEE Wireless Commun. Lett.*, vol. 9, no. 5, pp. 628–632, May 2020.

[9] P. Lai, H. Bai, Y. Huang, Z. Chen, and T. Liu, "Performance evaluation of underlay cognitive hybrid satellite–terrestrial relay networks with relay selection scheme," *IET Commun.*, vol. 13, no. 16, pp. 2550–2557, Oct. 2019.

[10] K. Guo, K. An, B. Zhang, Y. Huang, and G. Zheng, "Outage analysis of cognitive hybrid satellite-terrestrial networks with hardware impairments and multi-primary users," *IEEE Wireless Commun. Lett.*, vol. 7, no. 5, pp. 816–819, Oct. 2018.

[11] D.-T. Do, A.-T. Le, C.-B. Le, and B. M. Lee, "On exact outage and throughput performance of cognitive radio based non-orthogonal multiple access networks with and without D2D link," *Sensors*, vol. 19, no. 15, p. 3314, Jul. 2019.

[12] W. Shin, M. Vaezi, B. Lee, D. J. Love, J. Lee, and H. V. Poor, "Non-orthogonal multiple access in multi-cell networks: Theory, performance, and practical challenges," *IEEE Commun. Mag.*, vol. 55, no. 10, pp. 176–183, Oct. 2017.

[13] Z. Ding, Z. Yang, P. Fan, and H. V. Poor, "On the performance of non-orthogonal multiple access in 5G systems with randomly deployed users," *IEEE Signal Process. Lett.*, vol. 21, no. 12, pp. 1501–1505, Dec. 2014.

[14] X. Wang, J. Wang, L. He, and J. Song, "Outage analysis for downlink NOMA with statistical channel state information," *IEEE Wireless Commun. Lett.*, vol. 7, no. 2, pp. 142–145, Apr. 2018.

[15] H. E. Tan Zheng, A. S. Madhukumar, R. P. Sirigina, and A. K. Krishna, "An outage probability analysis of full-duplex NOMA in UAV communications," in *Proc. IEEE Wireless Commun. Netw. Conf. (WCNC)*, Apr. 2019, pp. 1–5.

[16] I. Cosandal, M. Koca, E. Biglieri, and H. Sari, "NOMA-2000 vs. PD-NOMA: An outage probability comparison," *IEEE Commun. Lett.*, vol. 25, no. 2, pp. 427–431, Feb. 2021, doi: 10.1109/LCOMM.2020.3033727.

[17] J. A. Oviedo and H. R. Sadjadpour, "A fair power allocation approach to NOMA in multiuser SISO systems," *IEEE Trans. Veh. Technol.*, vol. 66, no. 9, pp. 7974–7985, Sep. 2017.

[18] Y. Ji, W. Duan, M. Wen, P. Padidar, J. Li, N. Cheng, and P.-H. Ho, "Spectral efficiency enhanced cooperative device-to-device systems with NOMA," *IEEE Trans. Intell. Transp. Syst.*, early access, Jul. 17, 2020, doi: 10.1109/TITS.2020.3006857.

[19] A. Anwar, B.-C. Seet, S. F. Hasan, X. J. Li, P. H. J. Chong, and M. Y. Chung, "An analytical framework for multi-tier NOMA networks with underlay D2D communications," *IEEE Access*, vol. 6, pp. 59221–59241, 2018.

[20] D.-T. Do, A.-T. Le, and B. M. Lee, "NOMA in cooperative underlay cognitive radio networks under imperfect SIC," *IEEE Access*, vol. 8, pp. 86180–86195, 2020.

[21] L. Zhang, J. Liu, M. Xiao, G. Wu, Y.-C. Liang, and S. Li, "Performance analysis and optimization in downlink NOMA systems with cooperative full-duplex relaying," *IEEE J. Sel. Areas Commun.*, vol. 35, no. 10, pp. 2398–2412, Oct. 2017.

[22] D.-T. Do, T.-L. Nguyen, K. M. Rabie, X. Li, and B. M. Lee, "Throughput analysis of multipair two-way replaying networks with NOMA and imperfect CSI," *IEEE Access*, vol. 8, pp. 128942–128953, 2020.

[23] D.-T. Do and M.-S. Van Nguyen, "Device-to-device transmission modes in NOMA network with and without wireless power transfer," *Comput. Commun.*, vol. 139, pp. 67–77, May 2019.

[24] Z. Na, Y. Liu, J. Shi, C. Liu, and Z. Gao, "UAV-supported clustered NOMA for 6G-enabled Internet of Things: Trajectory planning and resource allocation," *IEEE Internet Things J.*, early access, Jun. 23, 2020, doi: 10.1109/JIOT.2020.3004432.

[25] W. Mei and R. Zhang, "Uplink cooperative NOMA for cellular-connected UAV," *IEEE J. Sel. Topics Signal Process.*, vol. 13, no. 3, pp. 644–656, Jun. 2019.

[26] D. Hu, Q. Zhang, Q. Li, and J. Qin, "Joint position, decoding order, and power allocation optimization in UAV-based NOMA downlink communications," *IEEE Syst. J.*, vol. 14, no. 2, pp. 2949–2960, Jun. 2020.

[27] S. Arzykulov, G. Nauryzbayev, T. A. Tsiftsis, and B. Maham, "Performance analysis of underlay cognitive radio nonorthogonal multiple access networks," *IEEE Trans. Veh. Technol.*, vol. 68, no. 9, pp. 9318–9322, Sep. 2019.

[28] L. Bariah, S. Muhaidat, and A. Al-Dweik, "Error performance of NOMA-based cognitive radio networks with partial relay selection and interference power constraints," *IEEE Trans. Commun.*, vol. 68, no. 2, pp. 765–777, Feb. 2020.

[29] L. Lv, L. Yang, H. Jiang, T. H. Luan, and J. Chen, "When NOMA meets multiuser cognitive radio: Opportunistic cooperation and user scheduling," *IEEE Trans. Veh. Technol.*, vol. 67, no. 7, pp. 6679–6684, Jul. 2018.

[30] W. Xu, X. Li, C.-H. Lee, M. Pan, and Z. Feng, "Joint sensing duration adaptation, user matching, and power allocation for cognitive OFDM-NOMA systems," *IEEE Trans. Wireless Commun.*, vol. 17, no. 2, pp. 1269–1282, Feb. 2018.

[31] V. Singh, P. K. Upadhyay, and M. Lin, "On the performance of NOMA-assisted overlay multiuser cognitive satellite-terrestrial networks," *IEEE Wireless Commun. Lett.*, vol. 9, no. 5, pp. 638–642, May 2020.

[32] V. Singh, V. Bankey, and P. K. Upadhyay, "Underlay cognitive hybrid satellite-terrestrial networks with cooperative-NOMA," in *Proc. IEEE Wireless Commun. Netw. Conf. (WCNC)*, May 2020, pp. 1–6.

[33] X. Zhang, D. Guo, K. An, Z. Chen, B. Zhao, Y. Ni, and B. Zhang, "Performance analysis of NOMA-based cooperative spectrum sharing in hybrid satellite-terrestrial networks," *IEEE Access*, vol. 7, pp. 172321–172329, 2019.

[34] V. Singh, S. Solanki, P. K. Upadhyay, D. B. da Costa, and J. M. Moualeu, "Performance analysis of hardware-impaired overlay cognitive satellite–terrestrial networks with adaptive relaying protocol," *IEEE Syst. J.*, vol. 15, no. 1, pp. 192–203, Mar. 2021, doi: 10.1109/JSYST.2020.2967836.

[35] P. K. Upadhyay and P. K. Sharma, "Max-max user-relay selection scheme in multiuser and multirelay hybrid satellite-terrestrial relay systems," *IEEE Commun. Lett.*, vol. 20, no. 2, pp. 268–271, Feb. 2016.

[36] K. An, J. Ouyang, M. Lin, and T. Liang, "Outage analysis of multi-antenna cognitive hybrid satellite-terrestrial relay networks with beamforming," *IEEE Commun. Lett.*, vol. 19, no. 7, pp. 1157–1160, Jul. 2015.

[37] I. S. Gradshteyn and I. M. Ryzhik, *Table of Integrals, Series, and Products*. New York, NY, USA: Academic, 2014.

[38] D. B. da Costa and S. Aissa, "Cooperative dual-hop relaying systems with beamforming over nakagami-m fading channels," *IEEE Trans. Wireless Commun.*, vol. 8, no. 8, pp. 3950–3954, Aug. 2009.

[39] X. Li, J. Li, and L. Li, "Performance analysis of impaired SWIPT NOMA relaying networks over imperfect weibull channels," *IEEE Syst. J.*, vol. 14, no. 1, pp. 669–672, Mar. 2020.

[40] V. S. Adamchik and O. I. Marichev, "The algorithm for calculating integrals of hypergeometric type functions and its realization in REDUCE system," in *Proc. Int. Symp. Symbolic Algebr. Comput. (ISSAC)*, Aug. 1990, pp. 212–224.

NHAT-TIEN NGUYEN was born in Ho Chi Minh City, Vietnam, in 1981. He received the B.Eng. degree from the Posts and Telecommunications Institute of Technology, in 2011, and the M.Eng. degree from the Ho Chi Minh City University of Technology, in 2017, with a focus on electrical engineering and telecommunications. He is currently pursuing the Ph.D. degree with the Technical University of Ostrava, Czech Republic. He is also a Lecturer with Sai Gon University, Vietnam. His research interests include wireless communications and network information theory.

HONG-NHU NGUYEN was born in Vietnam, in 1971. He received the B.Sc. degree in electronics engineering from the Ho Chi Minh City University of Technology, in 1998, and the M.Sc. degree in electronics engineering from the University of Transport and Communications, Vietnam, in 2012. He is currently pursuing the Ph.D. degree with the Technical University of Ostrava, Czech Republic. He is also working as a Lecturer with Sai Gon University. His research interests include applied electronics, wireless communications, cognitive radio, and energy harvesting.

NGOC-LONG NGUYEN was born in Vietnam, in August 1973. He received the B.S. and M.S. degrees in electric physics from the University of Science, Vietnam. He is currently pursuing the Ph.D. degree with the Technical University of Ostrava, Czech Republic. He is also working as a Lecturer with the Faculty of Applied Sciences, Ton Duc Thang University. His research interests include applied electronics, wireless communication, NOMA, cognitive radio, and energy harvesting.

ANH-TU LE was born in Vietnam, in 1997. He is currently pursuing the Ph.D. degree in communications and information system with a focus on wireless communications. He is also a Research Assistant with the WICOM Laboratory, led by Dr. Thuan. He has authored or coauthored five technical articles published in peer-reviewed international journals. His research interests include wireless channel modeling, NOMA, cognitive radio, and MIMO.

DINH-THUAN DO (Senior Member, IEEE) received the B.Sc., M.Eng., and Ph.D. degrees from Vietnam National University (VNU-HCMC), in 2003, 2007, and 2013, respectively, with a focus on communications engineering. From 2003 to 2009, he was a Senior Engineer with VinaPhone Mobile Network. From 2009 to 2010, he was a Visiting Ph.D. Student with the Communications Engineering Institute, National Tsing Hua University, Taiwan. He is a published author. He has authored or co-authored 95 technical articles published in peer-reviewed international journals (SCIE) and 70 other journal and conference papers. His research interests include signal processing in wireless communications networks, MIMO, NOMA, UAV networks, satellite systems, physical layer security, device-to-device transmission, and energy harvesting. He received the Golden Globe Award from the Vietnam Ministry of Science and Technology in 2015 (Top ten talented young scientists in Vietnam) and the Creative Young Medal in 2015. He has been lead guest editor of several special issues in peer-reviewed journals. He also serves as an Associate Editor in four leading SCIE journals.

MIROSLAV VOZNAK (Senior Member, IEEE) received the Ph.D. degree in telecommunications from the Faculty of Electrical Engineering and Computer Science, VSB-Technical University of Ostrava, in 2002, and the Habilitation degree in 2009. In 2017, he was appointed as a Full Professor in electronics and communications technologies. He has authored or coauthored over 100 articles indexed in SCI/SCIE journals. His research interests include information and communication technologies, quality of service and experience, network security, wireless networks, and big data analytics. According to the Stanford University study released in 2020, he is one of the World's Top 2% of Scientists in Networking and Telecommunications and Information and Communications Technologies.